

## OLIVINE RICH EXPOSURES IN BELLICIA AND ARRUNTIA CRATERS ON VESTA USING DAWN

FC. G. Thangjam<sup>1</sup>, A. Nathues<sup>1</sup>, K. Mengel<sup>2</sup>, M. Hoffmann<sup>1</sup>, M. Schäfer<sup>1</sup>, V. Reddy<sup>3,1</sup>, E.A. Cloutis<sup>4</sup>, U. Christensen<sup>1</sup>, H. Sierks<sup>1</sup>, L. Le Corre<sup>3</sup>, J. B. Vincent<sup>1</sup>, C. T. Russell<sup>5</sup>, C. Raymond<sup>6</sup>, <sup>1</sup>Max Planck Institute for Solar System Research, Katlenburg-Lindau, Germany, <sup>2</sup>Clausthal University of Technology, Clausthal-Zellerfeld, Germany, <sup>3</sup>Planetary Science Institute, Tucson, Arizona, USA, <sup>4</sup>University of Winnipeg, Canada, <sup>5</sup>University of California, Los Angeles, USA, <sup>6</sup>Jet Propulsion Laboratory, Pasadena, USA, (thangjam@mps.mpg.de).

**Introduction:** The Dawn Framing Camera (FC) [1] has imaged the entire visible surface of Vesta from three different orbits at spatial resolutions of ~250 m/pixel, ~60 m/pixel, and ~20 m/pixel. The FC is equipped with one clear and seven color filters, covering the wavelength range between 0.44 and 1.0  $\mu\text{m}$  [1].

Vesta is geologically the most diverse differentiated basaltic asteroid that survived the collisional history of the Solar System [2]. Most of the howardite-eucrite-diogenite meteorites (HEDs) and the Vestoids are believed to be samples from Vesta [3], [4]. Several models, based on the petrogenesis of HEDs [5], [6], favor the evolution of Vesta through a magma ocean. However, the variance of incompatible trace elements among diogenites also supports the serial magmatism model [7], [8]. The recent finding of olivine-rich exposures in Bellicia and Arruntia craters in the Northern Hemisphere [9], led to many ambiguities, as well as complexities in understanding the geological evolution of Vesta. Here we present our analyses and observations of two olivine-rich exposures.

**Band Parameters:** Spectra of HEDs, olivine-orthopyroxene mixtures, olivines, and high Ca-pyroxenes (HCPs) were acquired from RELAB, HOSERLab and USGS. The spectra were resampled to FC band-passes. HCPs are selected from low/high Ca-clinopyroxene [10], comparing the pyroxene composition to the reported HCPs in eucrites [11]. The olivine diagnostic FC parameters we have developed are:

$$\text{Band Tilt (BT)} = (R_{0.92\mu\text{m}} / R_{0.96\mu\text{m}})$$

$$\text{Mid Ratio (MR)} = (R_{0.75\mu\text{m}} / R_{0.83\mu\text{m}}) / (R_{0.83\mu\text{m}} / R_{0.92\mu\text{m}})$$

$$\text{Mid Curvature (MC)} = (R_{0.75\mu\text{m}} + R_{0.92\mu\text{m}}) / R_{0.83\mu\text{m}}$$

where  $R(\lambda)$  is the reflectance in the corresponding filter.

All band parameter values are plotted in the band parameter space BT versus MR, and BT versus MC. Polygons identified the different materials in the band parameter space (Fig. 1). BT is well suited to distinguish eucrites from diogenites [12], and values higher than 1.03 are absent for HEDs. However, a combination of the band parameters can be used to identify olivine-rich samples (>40% olivine).

**FC Data Processing:** FC images exist in three standard levels from which we use level 1c that is corrected for the “in-field” stray light component [13]. Level 1c I/F data is used for processing in our ISIS pipeline [14], which performs the photometric correc-

tion of the FC color data to standard viewing geometry using Hapke functions. The resulting reflectance data are map-projected in several steps, and co-registered to align the color frames, creating color cubes. For the present analysis, FC color data from HAMO and HAMO\_2 orbits were used. The color mosaics generated by the ISIS pipeline were analyzed using ENVI and ArcGIS software. For the photometric correction of our FC data and the visualization of the results, we used the Vesta shape model derived from FC clear filter images [15].

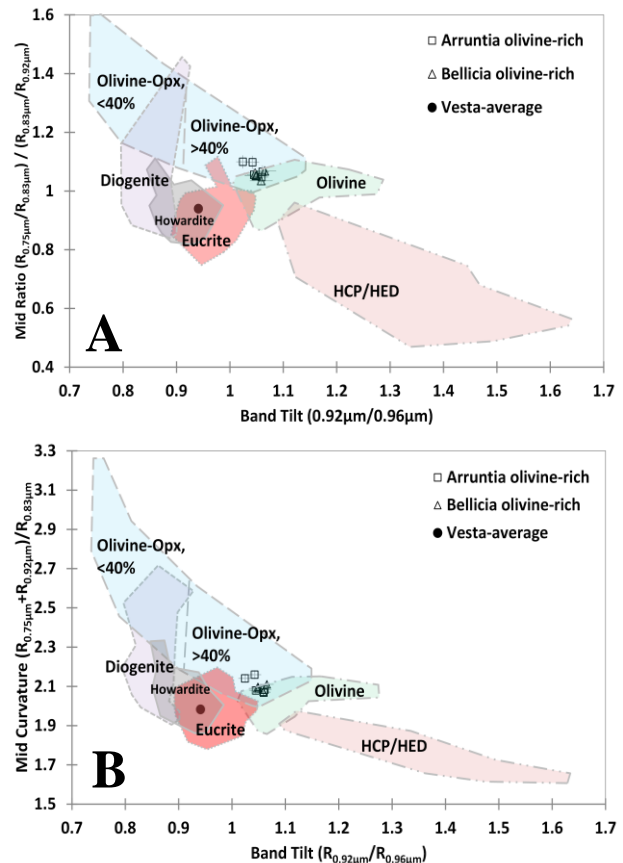


Fig. 1: Location of the Bellicia and Arruntia olivine-rich surface exposures in band parameter space, (A) BT versus MR, (B) BT versus MC. The polygons are based on our laboratory spectral analyses.

**FC Data Analysis:** The band parameters for Bellicia and Arruntia regions have been computed. RGB composites are prepared assigning BT as red, MR as green and MC as blue. The localities having higher

values in all the three parameters (white in RGB composites) are selected. The average spectra (2 x 2 pixels) of these localities are used to compute the band parameter values. The values are plotted in Fig. 1. The identified sites coincide with the nearly pure/olivine-rich regions, which implies that the identified sites are olivine-rich surface exposures. The potential olivine-rich exposures are shown as white patches in the RGB composites (Fig. 2). Fig. 3 shows the olivine-rich spectra normalized to 0.75  $\mu\text{m}$ . An average Vesta spectrum which is howarditic in nature is also shown.

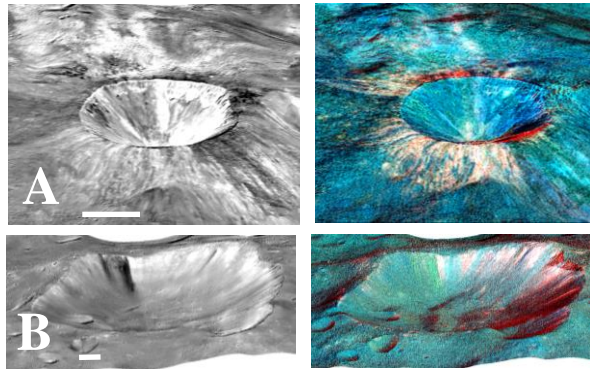


Fig. 2: Perspective view of the reflectance image (left) and RGB composites prepared assigning BT as red, MR as green, and MC as blue (right) for (A) Arruntia and (B) Bellicia-regions. Locations appearing white in the RGB composites are potential olivine-rich exposures. The perspective views are draped over HAMO-DTM ( $\sim 62$  m/pixel). North is up, and the scale bar shown in the image is 5 km in length.

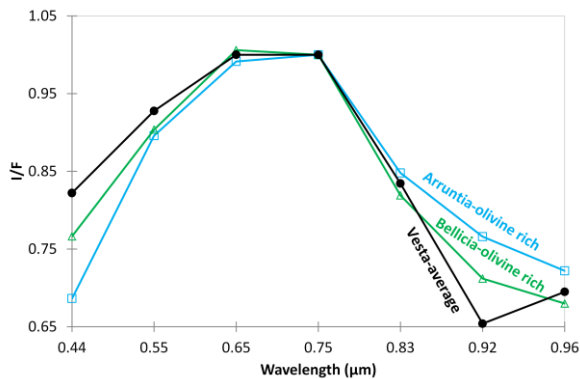


Fig. 3: Normalized spectra for olivine-rich exposures, and the average Vesta spectrum.

**Results and Discussion:** Based on our analyses, we have identified olivine-rich exposures in Bellicia and Arruntia craters. The size of the exposures extends a few hundreds of meters each. Despite FC datasets' limited spectral bands and wavelength range, the ob-

servations complements well the recent findings from hyperspectral VIR data [9].

The exposures could be distal ejecta from Rheasilvia basin as evidenced from the lithological signatures [16], [17], [18], cratering approach [19], [20], modeling of basin collisions on Vesta [21]. It also could be excavated materials from the nearby old basin, whose excavation depth is 10-15 km [19] assuming the crustal thickness of 15-20 km [22]. The exposures favor both the magma ocean and serial magmatism models [9]. A recent model of magma ocean crystallization followed by subsequent magmatic recharge [23] explains better the evolution of Vesta. A low concentration of olivine typically in the range of 10-30% on Vesta is hard to resolve spectrally [24]. The recent model [23] suggested non-excavation of olivine-rich mantle materials by the Rheasilvia impact, while the chondritic model [25] predicted a relatively pyroxene-rich mantle of Vesta. Meanwhile, the recent finding and mapping of potential olivine rich exposures on Vesta including few sites in the Rheasilvia basin [26] is significant to better understand the evolution of Vesta.

**References:** [1] Sierks H. et al. (2011) *Space Sci. Rev.*, 163, 263-327. [2] Russell C. T. et al. (2012) *Science*, 336, 684-686. [3] McCord T. B. et al. (1970) *Science*, 178, 745-747. [4] Schenck P. et al. (2012) *Science*, 336, 694-697. [5] Righter K. and Drake M. J. (1997) *Meteoritics & Planet. Sci.*, 32, 929-944. [6] Ruzicka A. et al. (1997) *Meteoritics & Planet. Sci.*, 32, 825-840. [7] Mittlefehldt D. W. (1994) *Geochim. Cosmochim. Acta*, 58, 1537-1552. [8] Fowler G. W. et al. (1995) *Geochim. Cosmochim. Acta*, 59, 3071-3084. [9] Ammanito E. et al. (2013) *Nature*, 504, 122-125. [10] Klima et al. (2011) *Meteoritics & Planet. Sci.*, 46, 379-395. [11] Mayne et al. (2009) *Geochim. et. Cosmochim.*, 73, 794-819. [12] Thangjam G. et al. (2013) *Meteoritics & Planet. Sci.*, 48, 2199-2210. [13] Kovacs G. et al. (2013) *Proc. SPIE* 8889. [14] Anderson J. A. et al. (2004) LPS XXXV, Abstract#2039. [15] Gaskell R. W. (2012) *AAS-DPS XLIV*, Abstract #209.03. [16] McSween H. Y. et al. (2013) *Meteoritics & Planet. Sci.*, 48, 2090-2104. [17] Ammanito E. et al. (2013) *Meteoritics & Planet. Sci.*, 48, 2185-2198. [18] Prettyman T. H. et al. (2013) *Meteoritics & Planet. Sci.*, 48, 2211-2236. [19] Marchi S. et al. (2012) *Science*, 336, 690-694. [20] Vincent J.-B. et al. *Planet. Space Sci.* (in press). [21] Jutzi M. et al. (2013) *Nature*, 494, 207-210. [22] Mandler B. E. and Elkins-Tanton L. T. (2013) *Meteoritics & Planet. Sci.*, 48, 2333-2349. [24] Beck et al. (2013) *Meteoritics & Planet. Sci.*, 48, 2155-2165. [25] Toplis M. J. et al. (2013) *Meteoritics & Planet. Sci.*, 48, 2300-2315. [26] Nathues A. et al. (2014) *LPS XLV*, (Abstract).